Prostaglandins, Leukotrienes and Essential Fatty Acids 196 (2023) 102585

Contents lists available at ScienceDirect

Prostaglandins, Leukotrienes and Essential Fatty Acids

journal homepage: www.elsevier.com/locate/plefa

Tumor microenvironment-derived monoacylglycerol lipase provokes tumor-specific immune responses and lipid profiles

Eva Gruden [a,1], Melanie Kienzl [a,1,*], Carina Hasenoehrl [a], Arailym Sarsembayeva [a], Dusica Ristic [a], Sophie Theresa Schmid [a], Kathrin Maitz [a], Ulrike Taschler [b], Lisa Hahnefeld [c,d], Robert Gurke [c,d], Dominique Thomas [c,d], Julia Kargl [a], Rudolf Schicho [a]

[a] Otto Loewi Research Center, Division of Pharmacology, Medical University of Graz, Austria
[b] Institute of Molecular Biosciences, University of Graz, Graz, Austria
[c] Institute of Clinical Pharmacology, Goethe University, 60590 Frankfurt/Main, Germany
[d] Fraunhofer Institute for Translational Medicine and Pharmacology ITMP, and Fraunhofer Cluster of Excellence for Immune Mediated Diseases CIMD, Theodor-Stern-Kai 7, 60596 Frankfurt am Main, Germany

ARTICLE INFO

Keywords:
Monoacylglycerol lipase
Tumor microenvironment
Endocannabinoids
(lyso)phospholipids
Melanoma
Non-small cell lung cancer

ABSTRACT

We recently described that monoacylglycerol lipase (MGL) is present in the tumor microenvironment (TME), increasing tumor growth. In this study we compare the implications of MGL deficiency in the TME in different tumor types.

We show that subcutaneous injection of KP ($Kras^{LSL\text{-}G12D}/p53^{fl/fl}$, mouse lung adenocarcinoma) or B16-F10 cells (mouse melanoma) induced tumor growth in MGL wild type (WT) and knockout (KO) mice. MGL deficiency in the TME attenuated the growth of KP cell tumors whereas tumors from B16-F10 cells increased in size. Opposite immune cell profiles were detected between the two tumor types in MGL KO mice. In line with their anti-tumorigenic function, the number of $CD8^+$ effector T cells and eosinophils increased in KP cell tumors of MGL KO vs. WT mice whereas their presence was reduced in B16-F10 cell tumors of MGL KO mice. Differences were seen in lipid profiles between the investigated tumor types. 2-arachidonoylglycerol (2-AG) content significantly increased in KP, but not B16-F10 cell tumors of MGL KO vs. WT mice while other endocannabinoid-related lipids remained unchanged. However, profiles of phospho- and lysophospholipids, sphingomyelins and fatty acids in KP cell tumors were clearly distinct to those measured in B16-F10 cell tumors.

Our data indicate that TME-localized MGL impacts tumor growth, as well as levels of 2-AG and other lipids in a tumor specific manner.

1. Introduction

Monoacylglycerol (or monoglyceride) lipase (MAGL, MGL) is a serine hydrolase that degrades monoglycerides including the endocannabinoid 2-arachidonoyl glycerol (2-AG) [1]. It is, therefore, part of the endocannabinoid system (ECS), a network of molecules that includes endocannabinoids (e.g. 2-AG), cannabinoid (e.g. CB_1 and CB_2) receptors, and enzymes for synthesis and degradation of endocannabinoids, maintaining homeostasis in many tissues [2]. In the brain, MGL generates arachidonic acid as precursor for the generation of neuroinflammatory prostaglandins [3]. Pharmacological blockade or genetic deletion of MGL reportedly leads to highly elevated 2-AG levels [4,5]. Apart from healthy tissue, components of the ECS, in particular, cannabinoid receptors, are found in various tumors [6]. Also, MGL has been detected in human tumor cells, such as ovarian, melanoma, lung, colon and prostate cancer cells [7–9], as well as in mouse cancer cells of lung adenocarcinoma (KP cells; isolated from a $Kras^{LSL\text{-}G12D}/p53^{fl/fl}$ mouse; [10]) and B16-F10 melanoma cells [11]. In human prostate cancer cells, MGL has been shown to regulate fatty acid (FA) metabolism and to enhance tumor aggressiveness by generating lipid species that contribute to tumor progression [7].

Studies in vivo models and human tissue have demonstrated that

* Corresponding author at: Otto-Loewi Research Center, Division of Pharmacology, Medical University of Graz, Neue Stiftingtalstrasse 6 (HBK M2 Ost), 8010 Graz, Austria
E-mail address: melanie.kienzl@medunigraz.at (M. Kienzl).
[1] These authors contributed equally

https://doi.org/10.1016/j.plefa.2023.102585
Received 26 April 2023; Received in revised form 2 August 2023; Accepted 8 August 2023
Available online 9 August 2023

MGL expression is mostly associated with tumor progression, like in melanoma [12], lung [10,13], colon [14] and endometrial cancer [15]. However, in vivo models of lung [16] and colon cancer [9] also revealed a tumor-suppressive role of MGL, suggesting that the involvement of MGL in tumor progression may be more complex than anticipated. In this context, we could show that MGL is not only present in tumor cells, but also in immune and stromal cells of the tumor microenvironment (TME), mostly in macrophages, fibroblasts and, to a lesser extent, in lymphocytes [10]. In a subcutaneous (s.c.) model of non-small cell lung cancer (NSCLC), deficiency of MGL in the TME reduced tumor growth generated by lung adenocarcinoma KP cells whereas overexpression of MGL in the KP cells enhanced tumor growth, indicating that tumor cell-derived as well as TME-cell derived MGL is involved in tumor progression [10]. We further detected increased levels of 2-AG in the tumors of MGL knockout (KO) vs. wild type (WT) mice [10]. 2-AG was able to induce the differentiation and migration of $CD8^+$ T cells, as well as the migration and activation of eosinophils indicating antitumorigenic effects of 2-AG via TME cells [10].

Following contradictory reports of MGL in the development of certain types of cancer, and the observation that fatty acids (FAs) and other lipids are regulated by MGL in tumor cells [7], we investigated whether the contribution of TME-derived MGL to tumor growth may be specific for a type of tumor and whether other lipid species beside endocannabinoids are regulated by TME-derived MGL. S.c. KP (mouse lung adenocarcinoma) cell tumors were compared with s.c. tumors from B16-F10 (mouse melanoma) cells in MGL WT and KO mice, i.e. in mice that expressed or lacked MGL within the TME cells. We further determined the immune cell composition of the TMEs by flow cytometry and measured the contents of several lipid species of the tumors by mass spectrometry.

2. Materials and methods

2.1. Animal studies and cell culture

All animal experiments were approved by the Austrian Federal Ministry of Science and Research (protocol number: BMBWF-66.010/0041-V/3b/2018) and performed in the animal facilities of the Medical University of Graz. MGL KO mice were a gift from Dr. R. Zimmermann [5] from the University of Graz and bred in-house together with wild-type (WT) littermates. The murine KP cell line (generously provided by Dr. McGarry Houghton) was isolated from a lung adenocarcinoma of a $Kras^{LSL\text{-}G12D}/p53^{fl/fl}$ mouse at the Fred Hutchinson Cancer Center (Seattle, WA, USA) after intratracheal administration of adenoviral Cre recombinase as previously described [17]. KP and B16-F10 cells (ATCC) were maintained in DMEM with 10% FBS (Life Technologies) and 1% penicillin/streptomycin (P/S, PAA Laboratories) at 37 °C and 5% CO_2 in a humidified atmosphere.

2.2. Tumor models

Parental KP and B16-F10 cells (0.5×10^6) were injected subcutaneously (s.c.) into the right flank of MGL WT or KO mice and allowed to grow for 2 weeks to form a tumor. Thereafter, tumors were collected for analysis, weighted, and measured with a caliper *ex vivo*. Tumor volume was calculated according to the following formula: v = length x width x height x $\pi/6$ [18].

2.3. Single-cell suspensions for flow cytometry

The preparation of single-cell suspensions from tumors was performed as previously described [10,18]. Using a scalpel, tumors were minced, and digested with DNase I (160 U/ml; Worthington) and collagenase (4.5 U/ml; Worthington) for 15 min at 37 °C while rotating at 1000 rpm. After brief vortexing, samples were incubated for 10 min before they were passed through a 40 μm cell strainer, washed in PBS+2% FBS, counted, and used for antigen staining.

2.4. Flow cytometric phenotyping of immune cell populations

First, single cell suspensions were incubated for 20 min in Fixable Viability Dye (FVD) eFluor™ 780 (eBioscience) in the dark on ice to exclude dead cells. After adding 1 μg TruStain™ FcX (Biolegend), immunostaining was performed on ice for 30 min (protected from light) with the following antibodies: CD45-AF700 (# 103,128), CD45-BV785 (# 103,149), Ly6C-APC (# 128,015), Ly6C-FITC (# 128,005), Ly6G-PE/Dazzle594 (# 127,648), CD11c-BV605 (# 117,334), CD8-PerCPCy5.5 (# 100,734), PD1-APC (# 135,210), CD62L-BV605 (# 104,438), CD44-FITC (# 103,005), CD19-FITC (# 115,506), CD19-PECy7 (# 115,520), PD1-BV421 (# 135,221) (all antibodies from Biolegend), and CD11b-BUV737 (# 612,801), F4/80-PE (# 565,410), Siglec-F-PerCP5.5 (# 565,526), F4/80-BUV395 (# 565,614), CD3-BUV395 (# 563,565), CD4-BUV496 (# 564,667), CD44-BUV737 (# 612,799), Siglec-F-PE (# 562,068) (all antibodies from BD Biosciences).

After staining, cells were washed and fixed using IC Fixation Buffer (eBioscience). Samples were either analyzed on a BD LSRFortessa™ or BD Canto II™ flow cytometer with FACSDiva software (BD Biosciences). Analyses and compensation were performed with Flowjo software (TreeStar). Fluorescence minus-one-samples were used to define gates. See Kienzl et al. [10] (Supplementary material) for gating strategies.

2.5. LC-MS analytics

Endocannabinoids and endocannabinoid-related lipids were determined in mouse tumor tissue using liquid chromatography in combination with tandem mass spectrometry as described previously in Gurke et al. [19]. Briefly, analysis was performed on a QTRAP 6500+ triple quadrupole mass spectrometer (Sciex, Darmstadt, Germany) equipped with a Turbo Spray ion source operated in positive electrospray ionization mode and coupled to an Agilent 1290 Infinity II UHPLC-system (Agilent, Waldbronn, Germany). Chromatographic separation was achieved using a binary gradient on an Acquity UPLC BEH C18 column (100 × 2.1 mm, 1.7 μm, Waters, Eschborn, Germany) with a pre-column of the same type. Details about the used equipment, materials, sample preparation, method parameters and a full list of analyzed endocannabinoids and related compounds have been previously published in Gurke et al. [19]. Additional lipids were analyzed from the tumor tissue sample using liquid chromatography coupled high-resolution mass spectrometry (LC—HRMS). All experimental details of the LC—HRMS lipid screening have been previously published in Hahnefeld et al. [20] The instrument setup consisted of a Nexera-X2 UHPLC system (Shimadzu, Kyoto, Japan) coupled to a TripleTOF 6600 with a DuoSpray ion source (both Sciex, Darmstadt, Germany) operated in both positive and negative ionization mode. Lipids were separated on a Zorbax RRHD Eclipse Plus C8 1.8 μm 50 × 2.1 mm ID column (Agilent, Waldbronn, Germany) with a precolumn of the same material. The compounds were detected using a MS1 screening from 100 – 1000 m/z with a mass resolving power of approximately 35,000 (mass error < 5 ppm) and further characterized using data-dependent acquisition of MS/MS spectra ranging from 50 – 1000 m/z with a collision energy of 40+/−20 V.

Tissue samples were prepared using wet grinding in a MixerMill MM400 (Retsch, Düsseldorf, Germany): to approximately 10 to 50 mg of tissue five zirconium dioxide balls and varying volumes of ethanol:water (1:3, v/v) were added and homogenized two times at 25 Hz for 2.5 min.

For analysis of endocannabinoids and related compounds a fixed volume of 800 μL ethanol:water (1:3, v/v) was added and 10, 100 and 200 μl of the resulting homogenate were filled to 200 μl with PBS if required and further extracted using ethyl acetate/hexane (9:1) as previously described [19].

For LC—HRMS lipid screening ethanol:water (1:3, v/v) was added to a tissue concentration of 0.05 mg/μl and 20 μl of the resulting

homogenate (equaling 1 mg of tissue) were extracted using liquid-liquid extraction with methyl-tert-butyl-ether and methanol as previously described [20]. LC—HRMS data acquisition and evaluation was done using Analyst TF software v1.7.1 and MultiQuant software v3.0.2 and the resulting chromatographic peak areas were normalized sample wise with the median peak ratio of the MarkerView software v.1.2.1 (all Sciex, Darmstadt, Germany) for positive and negative ionization mode, respectively.

2.6. Statistical analysis

Prism 9.3.1 (GraphPad® Software) was used to perform statistical analyses for in vitro and in vivo experiments. Gaussian distribution was tested by using Shapiro-Wilk normality test. Statistically significant differences between two experimental groups were determined using unpaired student's t-tests. Statistical analysis for not normally distributed data was performed using non-parametric Mann-Whitney tests. Lipid species data such as (lyso)phospholipids, sphingomyelins and FAs were analyzed in R (Version 4.0.3) using Welch's *t*-test, and plots of significantly different species were drawn with Prism 9.3.1 (GraphPad® Software). Measured levels of respective lipid species were normalized by defining smallest value in each data set as 0.0 and largest value in each data set as 1.0.

P values < 0.05 were considered significantly different and denoted with 1, 2 or 3 asterisks when lower than 0.05, 0.01 or 0.001, respectively.

3. Results

3.1. Opposing growth behavior of KP and B16-F10 cell tumors in MGL KO mice

MGL WT and KO mice were subcutaneously injected with either mouse KP lung adenocarcinoma or B16-F10 melanoma cells (Fig. 1A and C, respectively). After 14 days, tumors were collected and analyzed. As previously described [10], MGL KO mice bearing KP cell tumors showed reduced tumor weights and volumes (Fig. 1B), while in mice with B16-F10 tumors, weights and volumes were increased in comparison to tumors from WT mice (Fig. 1D).

3.2. MGL deficiency in the TME results in opposing immune cell profiles in KP and B16-F10 cell tumors

Flow cytometry of single cell suspensions from tumor samples revealed an increased percentage of $CD8^+$ T cells, in particular effector $CD8^+$ T cells ($CD8^+CD44^+$) and eosinophils in parallel with a decreased number of naïve $CD8^+T$ cells ($CD8^+CD62L^+$) and B cells in the TME of KP cell tumors of MGL KO vs. WT mice (Fig. 2A-H, [10]). In addition, PD-1 expression on $CD8^+$ T cells was higher in MGL KO than WT mice in KP cell tumors (Fig. 2B and C, [10]). In contrast, the number of $CD8^+$ T cells and $CD8^+$ effector T cells was reduced in B16-F10 cell tumors of MGL KO vs. WT mice while the population of naïve $CD8^+T$ cells and B cells was increased (Fig. 2A-F). Moreover, we observed a trend of decreased PD-1 expression on $CD8^+$ T cells from MGL KO compared to WT mice (Fig. 2B and C). Furthermore, we detected an increased infiltration of neutrophils and a trend in, but no significant reduction in eosinophils (Fig. 2G and H).

3.3. Lipid profiling revealed differences in endocannabinoid and (lyso) phospholipid levels

In line with our previous publication we only observed differences in endocannabinoid levels between MGL WT and KO mice for 2-arachidonoylglycerol (2-AG) but not for other endocannabinoid-related lipids, such as palmitoylethanolamide (PEA) and oleoylethanolamide (OEA) (Fig. 3A; [10]). In contrast to that no significant changes were seen in B16-F10 cell tumors in the measured endocannabinoids (Fig. 3B).

The differences between the tumor entities, e.g. in endocannabinoid levels and tumor development, led us to investigate potentially differential regulated lipid profiles. Thus, we performed lipid screening as described before [10,20] and identified several phospholipid and lysophospholipid species altered by MGL deficiency in the TME. The observed changes were dependent on the tumor type. B16-F10 cell tumors showed large changes in phospholipid content when compared to the KP cell tumors (Fig. 4A). KP cell tumors revealed a lysophospholipid profile that was entirely different from B16-F10 cell tumors (Fig. 4B). For example, our data showed that LPC was generally increased in KO vs. WT KP tumors and showed overall higher levels compared to B16-F10 tumors (Fig. 4B). Similarly, analyzed sphingomyelin content was elevated in KO vs. WT KP tumors and their abundance was

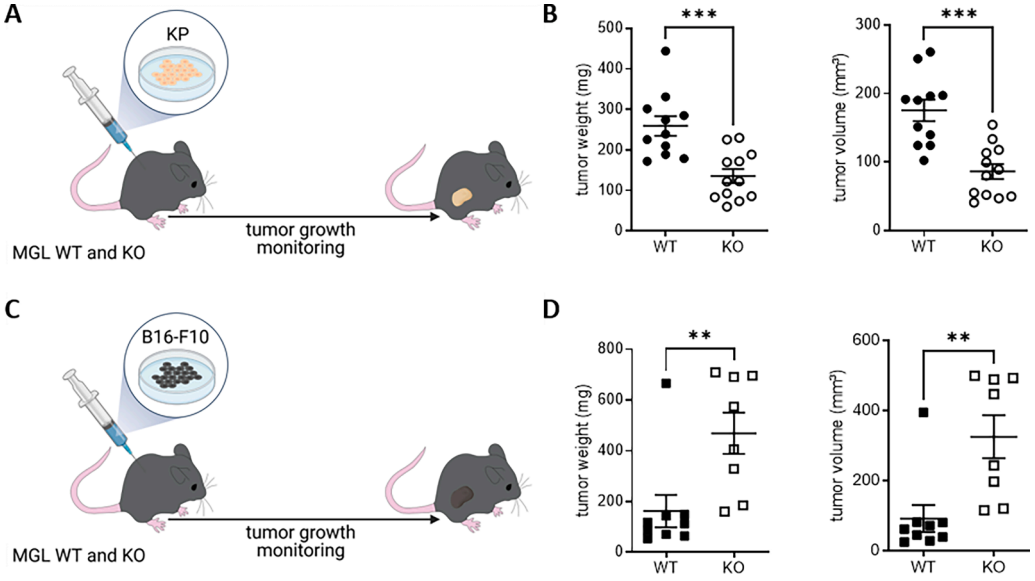

Fig. 1. Macroscopic evaluation of heterotopic KP and B16-F10 cell tumors. MGL wild type (WT) and knockout (KO) mice were injected subcutaneously either with (A) 5×10^5 KP (lung adenocarcinoma) or (C) B16-F10 (melanoma) cells and tumors were allowed to grow for 14 days post injection. (B, D) Tumor weights and volumes were measured *ex vivo* at the end of the experiment. Data indicate means ± SEM. Student's *t*-test; $n = 8–12$.

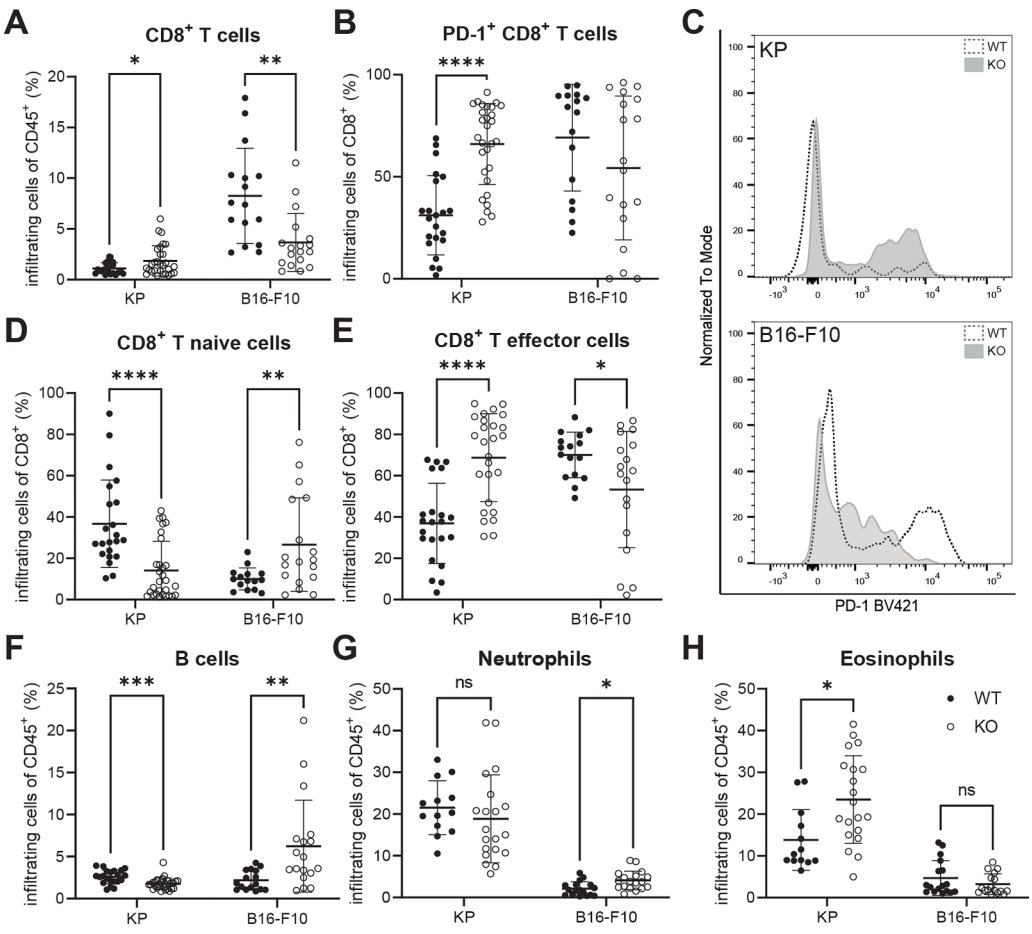

Fig. 2. Distinct immune cell profiles of KP and B16-F10 cell tumors in MGL knockout (KO) and wild type (WT) mice. Flow cytometric analysis of single cell suspensions of KP and B16-F10 cell tumors from MGL WT and KO mice (A-H). Data were pooled from 2 to 3 independent experiments. n = 19–30; (C) Representative histogram of PD-1 expression on CD8$^+$ T cells in KP and B16-F10 s.c. tumors of MGL WT (dotted white) or KO (gray) mice. Statistical differences were evaluated by multiple t-tests, $^*p \leq 0.05$, $^{**}p \leq 0.01$, $^{***}p \leq 0.001$, $^{****}p \leq 0.0001$, ns=not significant; data is shown as means ± SD.

noticeably reduced in B16-F10 tumors (Fig. 4C). Even though FA levels were lower in B16-F10 tumors compared to KP tumors, significant changes between WT and KO were observed there (Fig. 4D). In particular, there was no significant increase of arachidonic acid (C20:4) in KP cell tumors of MGL KO vs. WT whereas in B16-F10 cell tumors of MGL KO mice, C20:4 levels were significantly elevated (Fig. 4D). Lipid species with non-significant alterations are listed in supplementary Table 1.

4. Discussion

Components of the ECS, such as cannabinoid receptors and endocannabinoid-degrading enzymes (i.e. MGL and fatty acid amide hydrolase [FAAH]) have been widely investigated in several types of cancer and their impact in tumorigenesis was recently reviewed [21,22]. Many studies show that these enzymes are aberrantly expressed in tumor tissue (rev in [22]). High or low expression of the enzymes depends on the type of tumor and can correlate with either good or poor prognosis [22].

However, little is known about the role of the ECS in immune cells of the TME. Next to cannabinoid receptors [23], they contain endocannabinoid metabolizing enzymes, and they are able to produce and release endocannabinoids, thus forming an 'immune-endocannabinoid system' (rev in [24,25]). In the current study we investigated whether MGL present in the TME impacts tumor growth and whether this depends on the tumor type. Our s.c. tumor models demonstrated that TME-derived MGL has a tumor-promoting role in experimental NSCLC, but acts as a tumor suppressor in a melanoma model. Together with previous findings on the role of MGL in cancer cells [7,10,12,14] our data suggest that both tumor cell- and TME cell-derived MGL (and possibly also other components of the ECS) control tumor progression.

4.1. Differences in the immune cell profile between KP and B16-F10 cell tumors

Immune cells of the TME fundamentally influence the outcome of the tumor development [26,27]. For instance, a TME rich in tumor cell-killing CD8$^+$ T cells [28] favors tumor regression while low abundance of these cells is associated with a poor prognosis [26]. This matches our observation that KP cell tumors had, next to their smaller size, more CD8$^+$ T, CD8$^+$ T effector but less naïve CD8$^+$ T cells in MGL KO mice than in WT mice, while B16-F10 cell tumors showed the opposite. In our previous study [10] we described that these CD8$^+$ T cells highly express granzyme-B and interferon-γ, suggestive of increased tumoricidal activity. Similarly, the high expression of PD-1 on CD8$^+$ T cells in MGL KO mice also points towards increased immune cell activity in KP tumors [29], and, therefore, an antitumorigenic phenotype of CD8$^+$ T cells. In addition to CD8$^+$ T cells, our current data show opposing behavior of B cells, eosinophils, and neutrophils between the two tumor models. B cells have been described to have positive prognostic associations in lung adenocarcinoma and skin cutaneous melanoma [30]. Unexpectedly, B cells were decreased in the smaller KP tumors, whereas they were increased in the bigger B16-F10 tumors of MGL KO mice. Interestingly, 2-AG was described to positively regulate B cell homeostasis via CB_2 [31]. The role of B cells in the context of the ECS in cancer, however, is unclear [24]. Furthermore, presence of eosinophils tended to be reduced in B16-F10 cell tumors of MGL KO vs. WT mice, in parallel with larger tumors. Thus, our study is in accordance with Lucarini et al. who described an antitumorigenic role of eosinophils in B16-F10 melanoma [32]. On the other hand, the increased presence of eosinophils in KP cell tumors of MGL KO mice was accompanied by a reduction of tumor growth suggesting that presence of eosinophils in the

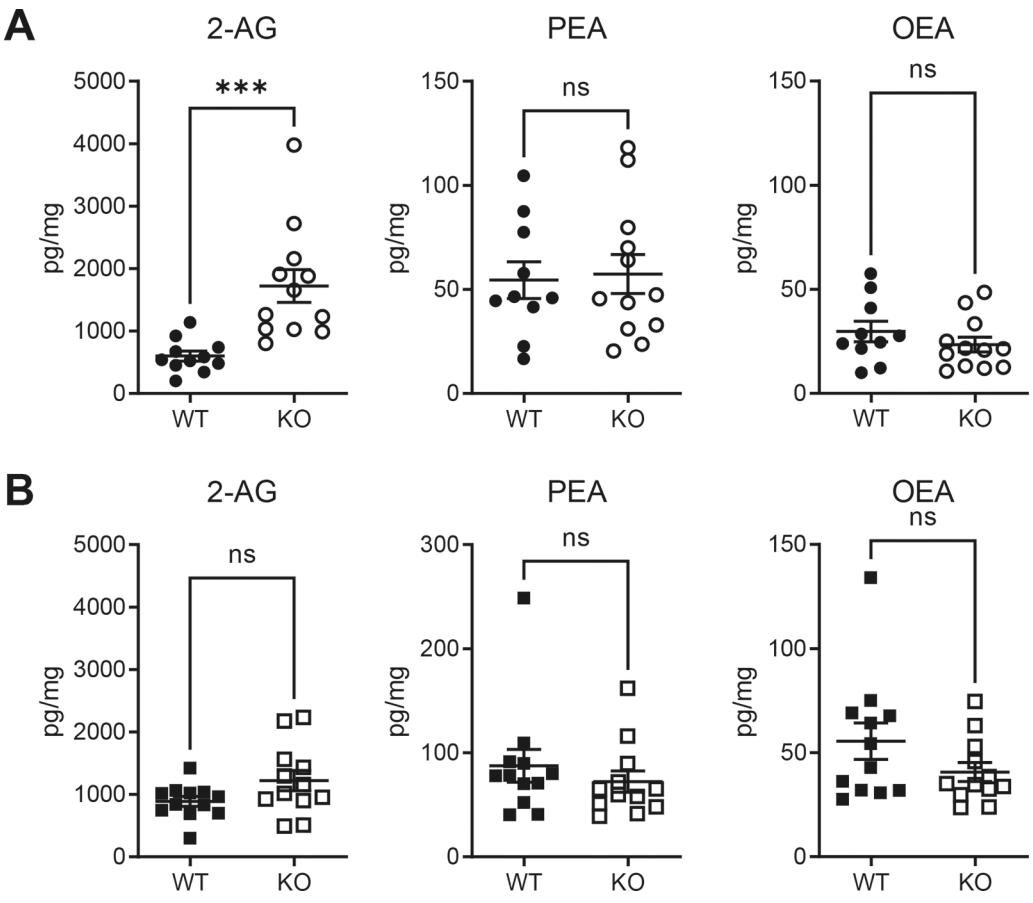

Fig. 3. Quantification of endocannabinoid and endocannabinoid-related lipids in KP and B16-F10 cell tumors from MGL WT and KO mice. KP (A) and B16-F10 (B) tumors were snap frozen in liquid nitrogen and tissue homogenates were prepared, lipids were extracted and subsequently analyzed with mass spectrometry. Statistically significant differences were assessed by using Student's *t*-test. $n = 11–12$. means ± SEM; *ns*, not significant (*2-AG*, 2-arachidonoylglycerol; *PEA*, palmitoylethanolamide; *OEA*, oleoylethanolamide).

TME could favor growth reduction in both types of cancers investigated. Neutrophils play an important role in the progression of lung cancer, especially in relation with $CD8^+$ T cells. In detail, an increased $CD8^+$ T cell to neutrophil ratio was associated with being indicative of improved response to immune checkpoint therapy [33], similarly the lymphocyte to neutrophil ratio seemed to be predictive for overall and progression free survival in melanoma patients [34]. Interestingly MGL absence is sufficient to drive potent changes by shaping the immune cell infiltration within (and between) different tumor entities, that results in differential regulation of cancer growth.

4.2. Endocannabinoids and endocannabinoid-related lipids

In our previous report we suggested that the increase of 2-AG in KP cell tumors of MGL KO vs. WT mice may have been a driver for the antitumorigenic behavior of $CD8^+$ T cells and eosinophils [10]. We reported that 2-AG promoted the shift from naïve $CD8^+$ T towards effector T cells in the MGL KO mice [10]. Contrarily, we could not detect a significant increase in 2-AG levels in B16-F10 tumors in MGL KO mice. No changes were observed in levels of other endocannabinoids. N-arachidonoylethanolamine (anandamide; AEA) levels were extremely low (data not shown) and often under the detection limit, therefore they likely play no role in the observed effects. In accordance with another study [35], our data corroborate the observation that 2-AG is involved in inhibiting tumor growth.

4.3. Differences in lipid profiles between KP and B16 cell tumors

Both KP and B16-F10 cell tumors show a clear distinction in lipid profiles. Nomura and coworkers have already reported that MGL not only controls 2-AG levels, but also those of FAs, prostaglandins and lysophospholipids which could promote tumor growth [7]. In our study, contents of phospholipids, lysophospholipids, FAs, and sphingomyelins show tumor specific patterns, indicating that MGL deficiency in TME cells leads to a reprograming of lipid production in the tumors. In general, lipid metabolism is highly adaptive in tumors [36]. Lipids may act as fuel for the energy demand of tumor cells, or they are needed to build up new membranes, as tumor cells proliferate [36]. Phospholipids represent another major part of membranes, and they were increased in B16-F10 tumors of MGL KO mice along with larger tumor sizes. However, certain phospholipid species also decreased in their content rather pointing to a high turnover than a mere increase of these lipids in B16-F10 tumors. Furthermore, lipids play an important role in regulating cell intrinsic pathways, as such, increased SM levels may interfere with the MAPK pathway and subsequently impair the cell cycle [37]. In line with our findings, Yang and colleagues discovered decreased LPC in malignant compared to benign pleural effusion [38]. Additionally, increased levels of saturated LPC 18:0 were identified to reduce the risk of most common cancers [39,40].

5. Conclusion

We have demonstrated that MGL derived from the TME controls the fate of KP and B16-F10 cell tumor growth in opposite ways. Tumor growth and immune cell response in a MGL-free TME is tumor type specific and indicates that TME-derived MGL can promote or suppress tumor growth. In addition, MGL in the TME strongly influences lipid profiles of the tumors which may have a bearing on tumor progression. As inhibitors of MGL and FAAH (AEA-degrading enzyme) have been recently suggested as new candidates for anti-tumor therapy [41] we should consider that blockade of MGL can affect both cancer cell- and TME cell-derived MGL, leading to tumor-specific outcomes. While

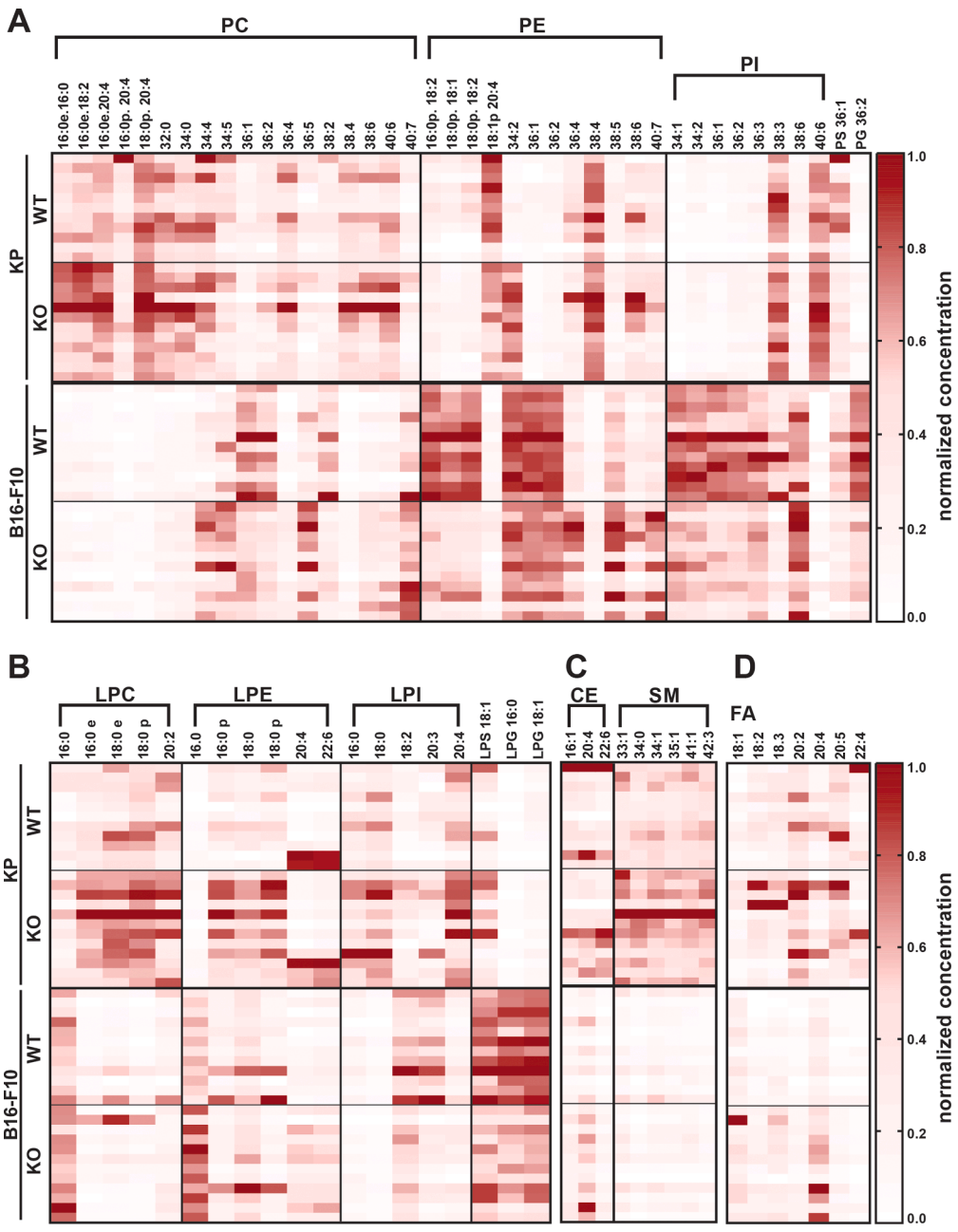

Fig. 4. Differential levels of lipid species of KP and B16-F10 cell tumors from MGL KO and wild type (WT) mice. Graphs show statistical significantly different lipid levels from mass spectrometry lipid screening of KP and B16-F10 cell tumors grown in MGL KO and WT mice ($n \geq 11$). Measured levels of respective lipid species were normalized by defining smallest value in each data set as 0.0 (white) and largest value in each data set as 1.0 (red): (A) Phospholipid, (B) lysophospholipid, (C) sphingomyelin and cholesteryl ester, and (D) fatty acid (FA). (CE, cholesteryl ester, PC, phosphatidylcholine; PE, phosphatidylethanolamine; PI, phosphatidylinositol; PS, phosphatidylserine; PG, phosphatidylglycerol; LPC, lysophosphatidylcholine; LPE, lysophosphatidylethanolamine; LPI, lysophosphatidylinositol; LPS, lysophosphatidylserine; LPG, lysophosphatidylglycerol; SM, sphingomyelin).

treatment of NSCLC patients with MGL inhibitors may be beneficial, it may be detrimental for patients with melanoma.

Funding details

The work was supported by grants of the Austrian Science Fund (FWF): P33325 and KLIF887 (RS)

Author contributions

MK, CH, JK and RS designed the experiments and supervised the study. MK, EG, CH, KM, AS, STS and DR.. participated in all the in vivo and in vitro experiments, collected data, and analyzed the results. MK, CH and EG did the statistical evaluation. LH, RG, and DT were responsible for the mass spectrometry experiments. MK, EG, CH, UT, JK, and RS interpreted the data and provided technical support. MK and RS participated in the writing of the manuscript. All authors critically revised and commented on the manuscript.

Declaration of Competing Interest

The authors report no conflict of interest

Acknowledgements

MK and EG receive funding from the Medical University of Graz (START). AS and DR were trained within the frame of the PhD Program *Molecular Medicine* of the Medical University of Graz. Work in the lab of JK is supported by the Austrian Science Fund (FWF) P35294. We are grateful to Veronika Pommer, Sabine Kern and Yannick Schreiber for their excellent technical assistance. Graphical abstract created with Biorender.com.

Supplementary materials

Supplementary material associated with this article can be found, in the online version, at doi:10.1016/j.plefa.2023.102585.

References

[1] G.F. Grabner, R. Zimmermann, R. Schicho, U. Taschler, Monoglyceride lipase as a drug target: at the crossroads of arachidonic acid metabolism and endocannabinoid signaling, Pharmacol. Ther. 175 (2017) 35–46, https://doi.org/10.1016/j.pharmthera.2017.02.033.

[2] V. Di Marzo, F. Piscitelli, The endocannabinoid system and its modulation by phytocannabinoids, Neurotherapeutics 12 (2015) 692–698, https://doi.org/10.1007/s13311-015-0374-6.

[3] D.K. Nomura, B.E. Morrison, J.L. Blankman, J.Z. Long, S.G. Kinsey, M.C. G. Marcondes, A.M. Ward, Y.K. Hahn, A.H. Lichtman, B. Conti, B.F. Cravatt, Endocannabinoid hydrolysis generates brain prostaglandins that promote neuroinflammation, Science 334 (2011) 809–813, https://doi.org/10.1126/science.1209200.

[4] J.E. Schlosburg, J.L. Blankman, J.Z. Long, D.K. Nomura, B. Pan, S.G. Kinsey, P. T. Nguyen, D. Ramesh, L. Booker, J.J. Burston, E.A. Thomas, D.E. Selley, L.J. Sim-Selley, Q. Liu, A.H. Lichtman, B.F. Cravatt, Chronic monoacylglycerol lipase blockade causes functional antagonism of the endocannabinoid system, Nat. Neurosci. 13 (2010) 1113–1119, https://doi.org/10.1038/nn.2616.

[5] U. Taschler, F.P.W. Radner, C. Heier, R. Schreiber, M. Schweiger, G. Schoiswohl, K. Preiss-Landl, D. Jaeger, B. Reiter, H.C. Koefeler, J. Wojciechowski, C. Theussl, J. M. Penninger, A. Lass, G. Haemmerle, R. Zechner, R. Zimmermann, Monoglyceride lipase deficiency in mice impairs lipolysis and attenuates diet-induced insulin resistance, J. Biol. Chem. 286 (2011) 17467–17477, https://doi.org/10.1074/jbc.M110.215434.

[6] R. Schicho, The endocannabinoid system in carcinogenesis. Mechanisms of Molecular Carcinogenesis–Volume 1, Springer, 2017, pp. 1–10.

[7] D.K. Nomura, D.P. Lombardi, J.W. Chang, S. Niessen, A.M. Ward, J.Z. Long, H. H. Hoover, B.F. Cravatt, Monoacylglycerol lipase exerts dual control over endocannabinoid and fatty acid pathways to support prostate cancer, Chem. Biol. 18 (2011) 846–856, https://doi.org/10.1016/j.chembiol.2011.05.009.

[8] J.L. Prüser, R. Ramer, F. Wittig, I. Ivanov, J. Merkord, B. Hinz, The monoacylglycerol lipase inhibitor JZL184 inhibits lung cancer cell invasion and metastasis via the CB1 cannabinoid receptor, Mol. Cancer Ther. 20 (2021) 787–802, https://doi.org/10.1158/1535-7163.MCT-20-0589.

[9] H. Sun, L. Jiang, X. Luo, W. Jin, Q. He, J. An, K. Lui, J. Shi, R. Rong, W. Su, C. Lucchesi, Y. Liu, M.S. Sheikh, Y. Huang, Potential tumor-suppressive role of monoglyceride lipase in human colorectal cancer, Oncogene 32 (2013) 234–241, https://doi.org/10.1038/onc.2012.34.

[10] M. Kienzl, C. Hasenoehrl, K. Maitz, A. Sarsembayeva, U. Taschler, P. Valadez-Cosmes, O. Kindler, D. Ristic, S. Raftopoulou, A. Santiso, T. Bärnthaler, L. Brcic, L. Hahnefeld, R. Gurke, D. Thomas, G. Geisslinger, J. Kargl, R. Schicho, Monoacylglycerol lipase deficiency in the tumor microenvironment slows tumor growth in non-small cell lung cancer, Oncoimmunology 10 (2021), 1965319, https://doi.org/10.1080/2162402X.2021.1965319.

[11] L. Hamtiaux, J. Masquelier, G.G. Muccioli, C. Bouzin, O. Feron, B. Gallez, D. M. Lambert, The association of N-palmitoylethanolamine with the FAAH inhibitor URB597 impairs melanoma growth through a supra-additive action, BMC Cancer 12 (2012), https://doi.org/10.1186/1471-2407-12-92, 92-2407-12–92.

[12] Y. Baba, T. Funakoshi, M. Mori, K. Emoto, Y. Masugi, S. Ekmekcioglu, M. Amagai, K. Tanese, Expression of monoacylglycerol lipase as a marker of tumour invasion and progression in malignant melanoma, J. Eur. Acad. Dermatol. Venereol. 31 (2017) 2038–2045, https://doi.org/10.1111/jdv.14455.

[13] H. Zhang, W. Guo, F. Zhang, R. Li, Y. Zhou, F. Shao, X. Feng, F. Tan, J. Wang, S. Gao, Y. Gao, J. He, Monoacylglycerol lipase knockdown inhibits cell proliferation and metastasis in lung adenocarcinoma, Front. Oncol. 10 (2020) 2781, https://doi.org/10.3389/fonc.2020.559568.

[14] L. Ye, B. Zhang, E.G. Seviour, K. Tao, X. Liu, Y. Ling, J. Chen, G. Wang, Monoacylglycerol lipase (MAGL) knockdown inhibits tumor cells growth in colorectal cancer, Cancer Lett. 307 (2011) 6–17, https://doi.org/10.1016/j.canlet.2011.03.007.

[15] X. Li, S. Gao, W. Li, Z. Liu, Z. Shi, C. Qiu, J. Jiang, Effect of monoacylglycerol lipase on the tumor growth in endometrial cancer, J. Obstet. Gynaecol. Res. 45 (2019) 2043–2054, https://doi.org/10.1111/jog.14070.

[16] R. Liu, X. Wang, C. Curtiss, S. Landas, R. Rong, M.S. Sheikh, Y. Huang, Monoglyceride lipase gene knockout in mice leads to increased incidence of lung adenocarcinoma, Cell Death Dis. 9 (2018) 1–15, https://doi.org/10.1038/s41419-017-0188-z.

[17] S.E. Busch, M.L. Hanke, J. Kargl, H.E. Metz, D. MacPherson, A.M. Houghton, Lung cancer subtypes generate unique immune responses, J.I 197 (2016) 4493–4503, https://doi.org/10.4049/jimmunol.1600576.

[18] M. Kienzl, C. Hasenoehrl, P. Valadez-Cosmes, K. Maitz, A. Sarsembayeva, E. Sturm, A. Heinemann, J. Kargl, R. Schicho, IL-33 reduces tumor growth in models of colorectal cancer with the help of eosinophils, Oncoimmunology 9 (2020), 1776059, https://doi.org/10.1080/2162402X.2020.1776059.

[19] R. Gurke, D. Thomas, Y. Schreiber, S.M.G. Schäfer, S.C. Fleck, G. Geisslinger, N. Ferreirós, Determination of endocannabinoids and endocannabinoid-like substances in human K3EDTA plasma – LC-MS/MS method validation and pre-analytical characteristics, Talanta 204 (2019) 386–394, https://doi.org/10.1016/j.talanta.2019.06.004.

[20] L. Hahnefeld, R. Gurke, D. Thomas, Y. Schreiber, S.M.G. Schäfer, S. Trautmann, I. F. Snodgrass, D. Kratz, G. Geisslinger, N. Ferreirós, Implementation of lipidomics in clinical routine: can fluoride/citrate blood sampling tubes improve preanalytical stability? Talanta 209 (2020), 120593 https://doi.org/10.1016/j.talanta.2019.120593.

[21] C. Laezza, C. Pagano, G. Navarra, O. Pastorino, M.C. Proto, D. Fiore, C. Piscopo, P. Gazzerro, M. Bifulco, The endocannabinoid system: a target for cancer treatment, Int. J. Mol. Sci. 21 (2020), https://doi.org/10.3390/ijms21030747.

[22] A.I. Fraguas-Sanchez, C. Martin-Sabroso, A.I. Torres-Suarez, Insights into the effects of the endocannabinoid system in cancer: a review, Br. J. Pharmacol. 175 (2018) 2566–2580, https://doi.org/10.1111/bph.14331.

[23] A. Sarsembayeva, M. Kienzl, E. Gruden, D. Ristic, K. Maitz, P. Valadez-Cosmes, A. Santiso, C. Hasenoehrl, L. Brcic, J. Lindenmann, J. Kargl, R. Schicho, Cannabinoid receptor 2 plays a pro-tumorigenic role in non-small cell lung cancer by limiting anti-tumor activity of CD8+ T and NK cells, Front. Immunol. 13 (2023). https://www.frontiersin.org/articles/10.3389/fimmu.2022.997115 (accessed April 25, 2023).

[24] M. Kienzl, J. Kargl, R. Schicho, The immune endocannabinoid system of the tumor microenvironment, Int. J. Mol. Sci. 21 (2020) 8929, https://doi.org/10.3390/ijms21238929.

[25] M. Iozzo, G. Sgrignani, G. Comito, P. Chiarugi, E. Giannoni, Endocannabinoid system and tumour microenvironment: new Intertwined connections for anticancer approaches, Cells 10 (2021) 3396, https://doi.org/10.3390/cells10123396.

[26] W.H. Fridman, F. Pagès, C. Sautès-Fridman, J. Galon, The immune contexture in human tumours: impact on clinical outcome, Nat. Rev. Cancer 12 (2012) 298–306, https://doi.org/10.1038/nrc3245.

[27] K. Pansy, B. Uhl, J. Krstic, M. Szmyra, K. Fechter, A. Santiso, L. Thuminger, H. Greinix, J. Kargl, K. Prochazka, J. Feichtinger, A.J. Deutsch, Immune regulatory processes of the tumor microenvironment under malignant conditions, Int. J. Mol. Sci 22 (2021), https://doi.org/10.3390/ijms222413311.

[28] L. Martinez-Lostao, A. Anel, J. Pardo, How do cytotoxic lymphocytes kill cancer cells? Clin. Cancer Res. 21 (2015) 5047–5056, https://doi.org/10.1158/1078-0432.CCR-15-0685.

[29] S. Simon, N. Labarriere, PD-1 expression on tumor-specific T cells: friend or foe for immunotherapy? Oncoimmunology 7 (2018), e1364828 https://doi.org/10.1080/2162402X.2017.1364828.

[30] C.M. Laumont, A.C. Banville, M. Gilardi, D.P. Hollern, B.H. Nelson, Tumour-infiltrating B cells: immunological mechanisms, clinical impact and therapeutic opportunities, Nat. Rev. Cancer 22 (2022) 414–430, https://doi.org/10.1038/s41568-022-00466-1.

[31] S. Basu, A. Ray, B.N. Dittel, Cannabinoid receptor 2 (CB2) is critical for the homing and retention of marginal zone B lineage cells and for efficient T-independent immune responses, J. Immunol. 187 (2011) 5720–5732, https://doi.org/10.4049/jimmunol.1102195.

[32] V. Lucarini, G. Zicchedda, I. Macchia, V. La Sorsa, F. Peschiaroli, C. Buccione, A. Sistigu, M. Sanchez, S. Andreone, M.T. D'Urso, M. Spada, D. Macchia, C. Afferni, F. Mattei, G. Schiavoni, IL-33 restricts tumor growth and inhibits pulmonary metastasis in melanoma-bearing mice through eosinophils, Oncoimmunology 6 (2017), https://doi.org/10.1080/2162402X.2017.1317420.

[33] J. Kargl, X. Zhu, H. Zhang, G.H.Y. Yang, T.J. Friesen, M. Shipley, D.Y. Maeda, J.A. Zebala, J. McKay-Fleisch, G. Meredith, A. Mashadi-Hossein, C. Baik, R.H. Pierce, M.W. Redman, J.C. Thompson, S.M. Albelda, H. Bolouri, A.M. Houghton, Neutrophil content predicts lymphocyte depletion and anti-PD1 treatment failure in NSCLC, JCI Insight. 4 (n.d.) e130850. https://doi.org/10.1172/jci.insight.130850.

[34] J.T. Cohen, T.J. Miner, M.P. Vezeridis, Is the neutrophil-to-lymphocyte ratio a useful prognostic indicator in melanoma patients?, Melanoma Manag. 7 (n.d.) MMT47. https://doi.org/10.2217/mmt-2020-0006.

[35] C. Qiu, L. Yang, B. Wang, L. Cui, C. Li, Y. Zhuo, L. Zhang, S. Zhang, Q. Zhang, X. Wang, The role of 2-arachidonoylglycerol in the regulation of the tumor-immune microenvironment in murine models of pancreatic cancer, Biomed. Pharmacotherapy 115 (2019), 108952, https://doi.org/10.1016/j.biopha.2019.108952.

[36] L.M. Butler, Y. Perone, J. Dehairs, L.E. Lupien, V. de Laat, A. Talebi, M. Loda, W. B. Kinlaw, J.V. Swinnen, Lipids and cancer: emerging roles in pathogenesis, diagnosis and therapeutic intervention, Adv. Drug Deliv. Rev 159 (2020) 245–293.

[37] R.Z. Li, X.R. Wang, J. Wang, C. Xie, X.X. Wang, H.D. Pan, W.Y. Meng, T.L. Liang, J. X. Li, P.Y. Yan, Q.B. Wu, L. Liu, X.J. Yao, E.L.H. Leung, The key role of sphingolipid metabolism in cancer: new therapeutic targets, diagnostic and prognostic values, and anti-tumor immunotherapy resistance, Front. Oncol. 12 (2022), 941643, https://doi.org/10.3389/fonc.2022.941643.

[38] Z. Yang, Z. Song, Z. Chen, Z. Guo, H. Jin, C. Ding, Y. Hong, Z. Cai, Metabolic and lipidomic characterization of malignant pleural effusion in human lung cancer, J. Pharm. Biomed. Anal. 180 (2020), 113069, https://doi.org/10.1016/j.jpba.2019.113069.

[39] E. Knuplez, G. Marsche, An updated review of pro- and anti-inflammatory properties of plasma lysophosphatidylcholines in the vascular system, Int. J. Mol. Sci. 21 (2020) 4501, https://doi.org/10.3390/ijms21124501.
[40] T. Kühn, A. Floegel, D. Sookthai, T. Johnson, U. Rolle-Kampczyk, W. Otto, M. von Bergen, H. Boeing, R. Kaaks, Higher plasma levels of lysophosphatidylcholine 18:0 are related to a lower risk of common cancers in a prospective metabolomics study, BMC Med. 14 (2016) 13, https://doi.org/10.1186/s12916-016-0552-3.
[41] S. Jaiswal, S.R. Ayyannan, Anticancer potential of small-molecule inhibitors of fatty acid amide hydrolase and monoacylglycerol lipase, ChemMedChem 16 (2021) 2172–2187, https://doi.org/10.1002/cmdc.202100120.